Transverse Vibration Characteristics of Clamped-Elastic Pinned Beam Under Compressive Axial Loads

Jianxun Zhang, Pengchong Zhang, Huicun Song, and Lei Zhu

Abstract Based on the Bernoulli–Euler theory, the vibration characteristics of a clamped-elastic pinned beam under the elastic constraint and the compressive axial loads are derived and verified by finite element method. The results of examples show that the natural frequency of the beam decreases with loads increase and the frequency increases with the increase of the elastic constraint stiffness. When the constraint stiffness increases from 10^4 to 10^8 N/m, the first-order natural frequency becomes 4.24 times, the second-order natural frequency becomes 2.19 times, and the third-order natural frequency becomes 1.57 times; when the constraint is weak, the loads change is mainly reflected in the first mode shape. When the constraint stiffness is 10^4 N/m, the first-order natural frequency decreases by 20%, the second-order modal natural frequency changes by 3%, and the third-order natural frequency changes by less than 1%. The range of the elastic constraints with significant changes in the natural frequencies of the higher-order modes is larger. When the first-order frequency is taken to $100EI/l^3$, the change tends to be flat, the second-order frequency is about five times that of the first-order, and the range of the third-order frequency is 15 times or more.

Keywords Clamped-elastic pinned beam · Compressive axial loads · Elastic constraint · Natural frequency · Mode · Finite element analysis

J. Zhang · P. Zhang · L. Zhu (✉)
School of Civil and Transportation Engineering, Beijing Key Laboratory of Functional Materials for Building Structure and Environment Remediation, Beijing Advanced Innovation Center for Future Urban Design, Beijing Higher Institution Engineering Research Center of Structural Engineering and New Materials, Beijing University of Civil Engineering and Architecture, Beijing 100044, China
e-mail: zhulei@bucea.edu.cn

H. Song
Culture Development Research Institute/School of Humanities, Beijing University of Civil Engineering and Architecture, Beijing 100044, China

Y. Yang (ed.), *Advances in Frontier Research on Engineering Structures*, Lecture Notes in Civil Engineering 286, https://doi.org/10.1007/978-981-19-8657-4_47

1 Introduction

A great deal of research work has been done on the natural vibration characteristics of beams under simple working conditions. In recent years, the research on beam structures under complex working conditions such as elastic restraint or axial load has been increasing gradually.

Clough and Penzien [1] gave the expressions of natural frequencies and mode functions of beams under various simple working conditions by solving the free vibration equation of transverse bending. Bokaian [2] proposed the natural frequencies and modes of beams under general boundary conditions under axial compression by solving analytical or semi-analytical solutions. Banerjee and Ananthapuvirajah [3] and Lee et al. [4] focused on the model itself and used different methods to analyze the free vibration of tapered beams. Murtagh et al. [5] simplified the research model into a beam structure, and numerically simulated the vibration characteristics of the structure by finite element method. Hu et al. [6] discussed the influence of axial pressure on the natural frequency of classical boundary beam structure and verified it by finite element method. Jafari et al. [7] analyzed the free vibration of Timoshenko beam by combining theory with finite element method. Chang et al. [8] studied the vibration characteristics of axially moving beams with fixed boundary conditions. Li [9] and Lin et al. [10] used the improved Fourier series method to study the free vibration of beams with general boundary conditions and elastic constraint boundary conditions. Zhao et al. [11] used the improved Fourier series method to study the influence of elastic constraint and axial load on the vibration characteristics of beams. Bao et al. [12] and Yang et al. [13] gave semi-analytical solutions of vertically elastically restrained beams for different models. The former considers the influence of variable cross-section, while the latter discusses the influence of constraint order. Wang [14] considered the influence of prestress effect on the natural frequency of beams. Zhang [15] and others simplified the wind turbine into a beam model and analyzed the theoretical solution and the finite element solution based on the beam element.

Considering that there is little research on the vibration characteristics of beams under the combined action of elastic constraint and external load, this paper analyzes the first three natural frequencies and corresponding vibration modes of beams by theoretical derivation and discusses the influence of constraint stiffness and axial compression load on the natural vibration characteristics of beams, which is verified by finite element method.

2 Theoretical Derivation

Figure 1 is a schematic diagram of the clamped-elastic pinned beam system, where EI is the equivalent bending stiffness of the beam ($N \times m^2$), m is the distributed mass of the beam (kg), k is the elastic constraint stiffness (N/m) in the y direction of the

Fig. 1 Clamped-elastic pinned beam system

hinge end, and the compressive axial loads F moves with the end, keeps horizontal and always acts on the geometric center line of the beam.

With Euler–Bernoulli beam model, it can be known that the transverse free vibration equation of the beam is a partial differential equation [1]:

$$\mathrm{m}(x)\frac{\delta^2 y(x,t)}{\delta t^2} + F\frac{\delta^2 y(x,t)}{\delta x^2} + \frac{\delta^2}{\delta x^2}\left[EI(x)\frac{\delta^2 y(x,t)}{\delta x^2}\right] = 0 \tag{1}$$

With the method of separating variables, the general solution of the equation is [1]:

$$y(x) = A\sin\ \delta x + B\cos\ \delta x + C\sinh\ \varepsilon x + D\cosh\ \varepsilon x \tag{2}$$

where A, B, C and D are constant coefficients, and δ and ε are defined as [1]:

$$\begin{aligned}\delta &= \left\{\left[\left(m\omega^2/EI\right) + (F/2EI)^2\right]^{1/2} + (F/2EI)\right\}^{1/2}\\ \varepsilon &= \left\{\left[\left(m\omega^2/EI\right) + (F/2EI)^2\right]^{1/2} - (F/2EI)\right\}^{1/2}\end{aligned} \tag{3}$$

The deformation of the system belongs to linear elastic small deformation motion, and the boundary condition of the fixed end is:

$$\begin{aligned}&[y(x,t)]_{x=0} = 0;\\ &\left[\frac{\partial y(x,t)}{\partial x}\right]_{x=0} = 0\end{aligned} \tag{4}$$

Considering the influence of forces generated by rotation angle and displacement at the elastic hinge supporting end, the boundary condition is:

$$\begin{aligned}&\left[\frac{\partial^2 y(x,t)}{\partial x^2}\right]_{x=l} = 0;\\ &\left[\frac{\partial^3 y(x,t)}{\partial x^3} + (F/EI)\frac{\partial y(x,t)}{\partial x}\right]_{x=l} = [-(k/EI)y(x,t)]_{x=l}\end{aligned} \tag{5}$$

Substituting formula (4) into formula (2), we obtained the following equations:

$$\begin{aligned}&[y(x,t)]_{x=0} = B + D = 0;\\&\left[\frac{\partial y(x,t)}{\partial x}\right]_{x=0} = \delta A + \varepsilon C = 0\end{aligned} \tag{6}$$

Substituting formula (5) into formula (2), we obtained the following equations:

$$\begin{aligned}\left[\frac{\partial^2 y(x,t)}{\partial x^2}\right]_{x=l} &= -A\delta^2 \sin\delta l - B\delta^2 \cos\delta l\\&\quad + C\varepsilon^2 \sinh\varepsilon l + D\varepsilon^2 \cosh\varepsilon l = 0;\\&\left[\frac{\partial^3 y(x,t)}{\partial x^3} + (F/EI)\frac{\partial y(x,t)}{\partial x} + (k/EI)y(x,t)\right]_{x=l}\\&= -A\delta^3 \cos\delta l + B\delta^3 \sin\delta l + C\varepsilon^3 \cosh\varepsilon l + D\varepsilon^3 \cosh\varepsilon l\\&+ (F/EI)(A\delta \cos\delta l - B\delta \sin\delta l + C\varepsilon \cosh\varepsilon l + D\varepsilon \sinh\varepsilon l)\\&+ (k/EI)(A \sin\delta l + B \cos\delta l + C \sinh\varepsilon l + D \cosh\varepsilon l) = 0\end{aligned} \tag{7}$$

Then substitute formula (6) into formula (7), and keep A and B to get:

$$\begin{aligned}&A\left(-\delta^2 \sin\delta l - \delta\varepsilon \sinh\varepsilon l\right) + B\left(-\delta^2 \cos\delta l - \varepsilon^2 \cosh\varepsilon l\right) = 0\\&A\left[-\delta^3 \cos\delta l - \delta\varepsilon^2 \cosh\varepsilon l + (F/EI)(\delta \cos\delta l - \delta \cosh\varepsilon l)\right.\\&\left.+ (k/EI)(\sin\delta l - \delta/\varepsilon \sinh\varepsilon l)\right] + B\left[\delta^3 \sin\delta l - \varepsilon^3 \sinh\varepsilon l\right.\\&\left.+ (F/EI)(-\delta \sin\delta l - \varepsilon \sinh\varepsilon l) + (k/EI)(\cos\delta l - \cosh\varepsilon l)\right] = 0\end{aligned} \tag{8}$$

Equation (8) should have a non-zero solution, therefore, it is impossible for both A and B to be 0, then the corresponding determinant is 0, which can be solved as:

$$\begin{aligned}&\delta\varepsilon\left[2\delta^2\varepsilon^2 - \delta\varepsilon\left(\delta^2 - \varepsilon^2\right)\sin\delta l \sinh\varepsilon l + \left(\delta^4 + \varepsilon^4\right)\cos\delta l \cosh\varepsilon l\right]\\&+k/EI\left(\delta^2 + \varepsilon^2\right)(\varepsilon \sin\delta l \cosh\varepsilon l - \delta \cos\delta l \sinh\varepsilon l) = 0\end{aligned} \tag{9a}$$

If we introduce the definitions of U = N/(2EI) and $\Omega = \omega\,(m/EI)^{1/2}$, there are:

$$\delta^4 + \varepsilon^4 = 4U^2 + 2\Omega^2;\ \delta^2 - \varepsilon^2 = 2U;\ \delta\varepsilon = \Omega \tag{10}$$

The formula (9a) can be reduced to:

$$\begin{aligned}&2\delta\varepsilon\left[\Omega^2 - U\Omega \sin\delta l \sinh\varepsilon l + \left(2U^2 + \Omega^2\right)\cos\delta l \cosh\varepsilon l\right]\\&+k/EI\left(\delta^2 + \varepsilon^2\right)(\varepsilon \sin\delta l \cosh\varepsilon l - \delta \cos\delta l \sinh\varepsilon l) = 0\end{aligned} \tag{9b}$$

When k approaches 0, the system becomes a cantilever beam system under compressive axial loads, and the natural frequency characteristic equation is equivalent to:

$$\Omega^2 - U\Omega \sin \delta l \sinh \varepsilon l + \left(2U^2 + \Omega^2\right) \cos \delta l \cosh \varepsilon l = 0 \quad (11)$$

The formula is the same as that of the cantilever beam frequency equation in reference [3].

When k tends to infinity, the system becomes a clamped-elastic pinned beam system under compressive axial loads, and the natural frequency characteristic equation is equivalent to:

$$\varepsilon \sin \delta l \cosh \varepsilon l - \delta \cos \delta l \sinh \varepsilon l = 0 \quad (12)$$

The formula is the same as the result given in reference [5].

The frequency characteristic Eq. (9a) is a transcendental equation, and only its numerical solution can be obtained instead of analytical solution. After obtaining the natural frequency, we can obtaine the mode function by formula (8).

We may as well set C = 1, and we can get from the first equation in Eqs. (6) and (8):

$$\begin{aligned} A &= -\varepsilon/\delta;\ B = \frac{\delta\varepsilon \sin \delta l + \varepsilon^2 \sinh \varepsilon l}{\delta^2 \cos \delta + \varepsilon^2 \cosh \varepsilon}; \\ C &= 1;\ D = -\frac{\delta\varepsilon \sin \delta l + \varepsilon^2 \sinh \varepsilon l}{\delta^2 \cos \delta + \varepsilon^2 \cosh \varepsilon}; \end{aligned} \quad (13)$$

The coefficients in the formula do not include k, and the influence of elastic constraint stiffness on the mode shape is reflected by the natural frequency value. These coefficients can also be deduced from the second equation in Eq. (8), and although they are expressed in different forms, their values are the same.

3 Verification

3.1 Model Establishment

In order to verify the reliability of the theoretical derivation in this paper, the finite element method is used to carry out numerical calculation, and the model data of different scales are compared. A 137-m-high circular section tower was selected as the analysis object, and the general finite element software ABAQUS was used for analysis. In engineering analysis, the model can be simplified into a beam model, where the outer diameter and inner diameter of the tower are 4.28 and 4.23 m, the material is steel, the elastic modulus is 2.1×10^{11} N/m^2, the Poisson's ratio is 0.3, the density is 7850 kg/m^3, and the critical load of Euler under cantilever state is about 2.05×10^7 N.

The B21 Euler beam element was chosen to establish the beam model, and the effects of shear deformation and moment of inertia were ignored. The whole beam

Fig. 2 Finite element model of beam

was divided into 20 elements and a total of 21 nodes. Considering the request of modal number was limited, the subspace iteration method was used to solve the natural frequency. The finite element model is shown in Fig. 2.

3.2 Calculation of Natural Frequency

Considering that in practical engineering, the structure may be unstable if the axial load reaches the critical load, the range of compressive axial loads variation is set as 0 N to 2.05×10^7 N, and the maximum value corresponds to the Euler critical load of the first mode shapes of the cantilever beam. The comparison of natural frequencies obtained from different elastic constraint stiffness values and compressive axial loads values is shown in Table 1.

As can be seen from Table 1, the natural frequency value derived by the method in this paper is very close to the value obtained by the finite element method, with an error of less than 1%, which verifies the theoretical solution.

The data in Table 1 show that the natural frequency values corresponding to the first three modes of the structure decrease with the increase of the compressive axial loads under these constraints. The higher the order corresponding to the natural frequency is, the smaller the influence brought by the axial loads is. When the compressive axial loads change from 0 to half of Euler critical load, the maximum range of first-order frequency can reach 25.96%, the maximum value of second-order frequency is 4.20%, and the third-order frequency is 1.26%. At the same time, it can be seen that the stronger the top elastic constraint is, the smaller the influence of compressive axial loads with the same amplitude will be. When the constraint is raised from 10^4 to 10^8 N/m, the variation range of the first-order frequency is reduced to 2.95%, and the variation range of the second-order and third-order frequency is less than 1%.

The influence of compressive axial loads and elastic constraint on natural frequency is further discussed below, and only the first order frequency with obvious change is concerned. Figure 3 shows the change trend of natural frequency with the increase of restraint stiffness when the compressive axial loads is set. It can be seen that with the increase of the elastic restraint stiffness, the natural frequency also rises, but the rising rate gradually slows down.

Figure 4 shows the variation trend of natural frequency with the increase of compressive axial loads when the constraint stiffness is fixed. It can be seen that the natural frequency decreases with the increase of compressive axial loads, and the rate of decline gradually accelerates, which is consistent with the conclusion in

Table 1 Comparison of finite element method and equations

Rigidity k/(N/m)	Axial loads F/(N/m)	First order natural frequency			Second order natural frequency			Third order natural frequency		
		Natural frequency/Hz		Relative error (%)	Natural frequency/Hz		Relative error (%)	Natural frequency/Hz		Relative error (%)
		Theory	FEA		Theory	FEA		Theory	FEA	
10^4	0	1.4977	1.4977	−0.002	9.1517	9.1515	0.003	25.6099	25.6103	−0.001
	1.02E + 07	1.1089	1.1089	−0.002	8.7677	8.7676	0.002	25.2884	25.2886	−0.001
	2.05E + 07	0.3508	0.3511	−0.098	8.3605	8.3604	0.001	24.9596	24.9600	−0.001
10^5	0	1.8023	1.8023	0.002	9.2082	9.2080	0.002	25.6300	25.6297	0.001
	1.02E + 07	1.5101	1.5102	−0.004	8.8255	8.8254	0.002	25.3086	25.3087	0.000
	2.05E + 07	1.1087	1.1088	−0.008	8.4195	8.4195	0.000	24.9798	24.9801	−0.001
10^6	0	3.4259	3.4259	0.000	9.8068	9.8068	0.000	25.8349	25.8352	−0.001
	1.02E + 07	3.3265	3.3265	0.000	9.4463	9.4461	0.002	25.5147	25.5148	0.000
	2.05E + 07	3.2210	3.2209	0.002	9.0632	9.0635	−0.003	25.1871	25.1874	−0.001
10^7	0	5.8388	5.8387	0.001	14.8719	14.8717	0.002	28.2447	28.2448	0.000
	1.02E + 07	5.7045	5.7044	0.001	14.7077	14.7077	0.000	27.9592	27.9595	−0.001
	2.05E + 07	5.5610	5.5609	0.001	14.5407	14.5405	0.001	27.6672	27.6674	−0.001
10^8	0	6.3428	6.3429	−0.001	20.0786	20.0785	0.000	40.0798	40.0811	−0.003
	1.02E + 07	6.1559	6.1558	0.002	19.8803	19.8800	0.002	39.8939	39.8951	−0.003
	2.05E + 07	5.9601	5.9600	0.001	19.6775	19.6777	−0.001	39.7048	39.7060	−0.003

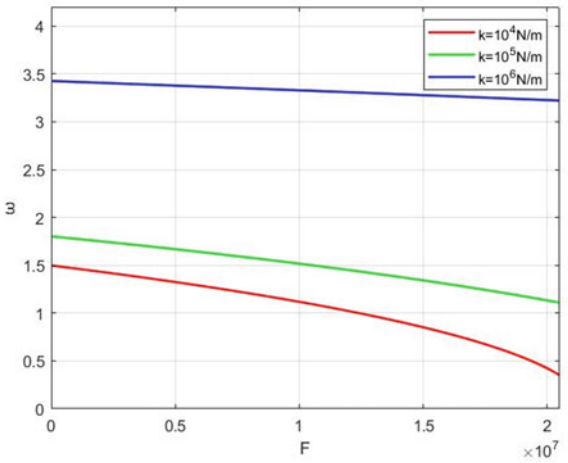

Fig. 3 Relationship between constraint stiffness and natural frequency

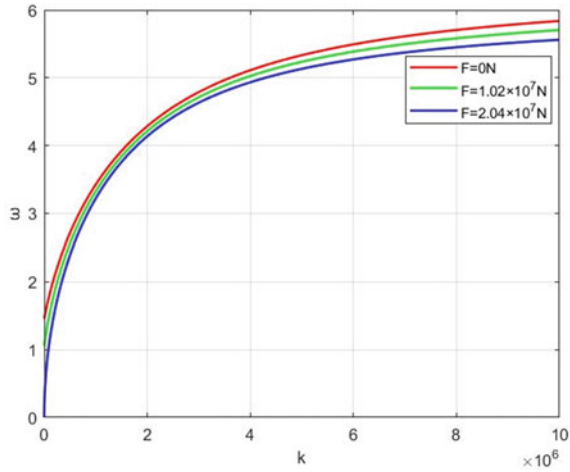

Fig. 4 Relationship between axial load stiffness and natural frequency

reference [2]. At the same time, it can be noticed that when the elastic constraint takes a small value, the decline rate is faster; when the value is larger, the decline rate is relatively slower, which is consistent with the change trend shown in Table 1.

3.3 Modes Analysis

The transverse bending mode shapes of the tower are obtained by modal analysis in ABAQUS. In order to study the influence of the number of divided elements on the results, the displacement of the node of the beam divided into 5 elements is used. Compared with the results of 20 elements, the maximum error of the natural

frequency value is 1.02%. Compared with the theoretical results obtained in Eqs. (2), (3) and (13), the first three bending modes are shown in Figs. 5 and 6.

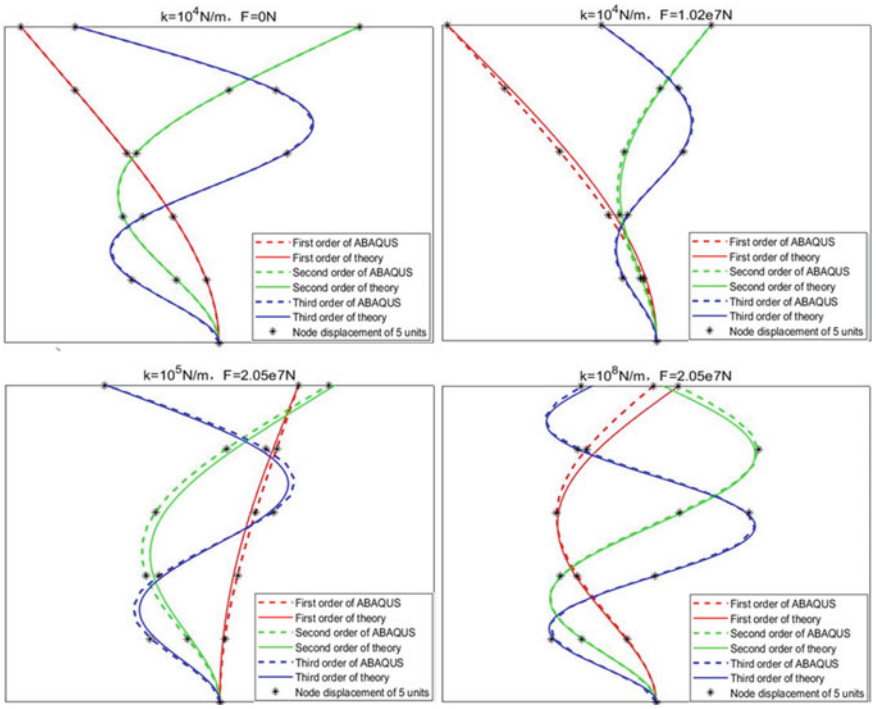

Fig. 5 Comparison of the first three modes of finite element and theoretical solution

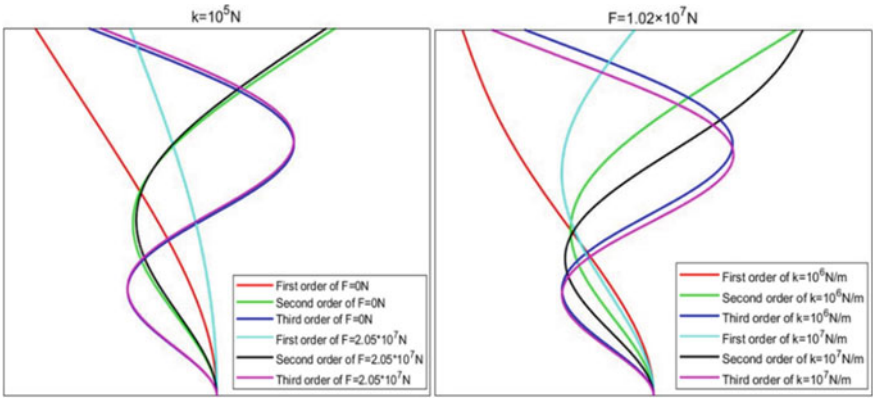

Fig. 6 Comparison of the first three modes derived from theory

It can be seen that the influence of compressive axial loads on the first mode is more significant than that on the higher mode, and the elastic constraint also has a more obvious influence on the higher mode.

3.4 *Influence of Coupling of Constrained Stiffness and Compressive Axial Loads on Natural Frequency*

As can be seen from the above results, the degree of influence of axial pressure on structural vibration characteristics decreases significantly with the increase of constraint stiffness, and the higher order mode is not sensitive to the change of axial pressure. This may be due to the different critical loads corresponding to the different modes of the calculation model. The larger the critical load is, the smaller the modal change caused by compressive axial loads with the same change amplitude is. Considering that the parameters of different beams are different, the constraints stiffness, axial pressure and natural frequency are dimensionlessly processed in the following analysis. Each parameter is written as:

$$F = aP_{cr} \qquad k = b\frac{EI}{l^3} \qquad \omega = c\sqrt{\frac{EI}{ml^4}} \tag{14}$$

In the formula, a is a constant with a value between 0 and 1, and Pcr is the first order Euler critical load of the structure under the cantilever beam condition; b and c are constants with values greater than 0.

The influence of the constraint stiffness and the compressive axial loads on the natural frequencies of the beam is as follows:

As can be seen from Fig. 7, compared with the low-order modes, the elastic constraint value range of the natural frequency of the high-order modes with significant changes is larger. When the first order frequency reaches $100EI/l^3$, the change tends to be gentle; when the second order frequency reaches $500EI/l^3$, the change tends to be gentle; and the third order frequency will gradually gentle when it reaches over $1500EI/l^3$. Theoretically speaking, the natural frequency will not increase infinitely with the increase of constraint stiffness. Finally, when the constraint stiffness is large, the elastic end displacement is small, and the structure can be approximated as a clamped-elastic pinned beam. In addition, it can be seen from the figure that when the axial compression is not greater than the first-order Euler critical load, its influence on the natural frequency of the structure is mainly reflected in the first-order modes, but it is not obvious in the higher-order modes, and the natural frequency of the second and third order modes decreases by no more than 10%.

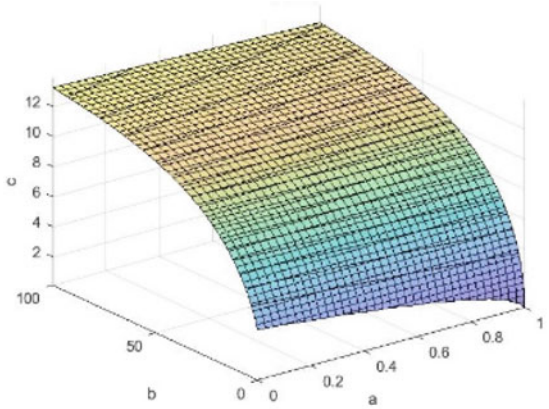

The first order mode

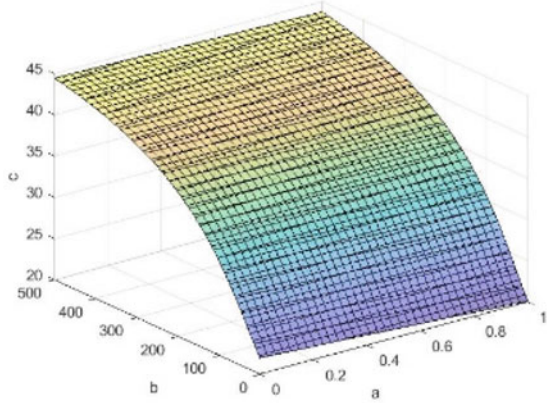

The second order mode

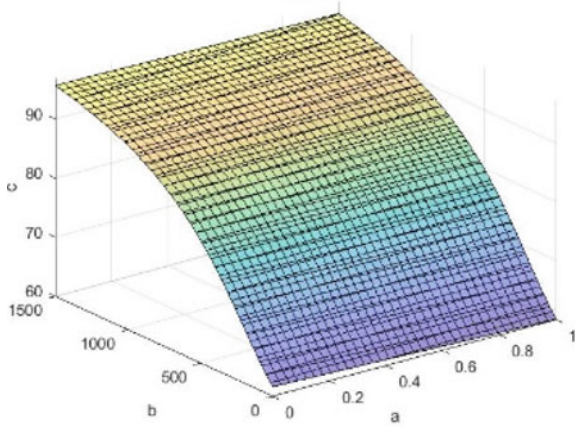

The third order mode

Fig. 7 Influence of coupling of axial pressure and constraint stiffness on the first three modes

4 Conclusions

In this paper, theoretical derivation and finite element method are used to study the vibration characteristics of clamped-elastic pinned beams, and the following conclusions are drawn:

(1) Based on the Euler beam theory, the natural frequency characteristic equation and mode shape expression of the clamped-elastic pinned beam are obtained and verified by finite element analysis.
(2) When the compressive axial load on the beam increases, the beam's natural frequency decreases, and the first-order frequency decreases from 2.95 to 25.96% corresponding to 0–50% Euler critical load under different elastic restraint stiffness. When the lateral elastic restraint stiffness of the elastic end of the beam increases, the natural frequency increases. When the restraint stiffness increases from 10^4 to 10^8 N/m, the first natural frequency becomes 4.24 times, the second natural frequency becomes 2.19 times and the third natural frequency becomes 1.57 times.
(3) When the elastic end constraint of the beam is strong, the change of axial compression in a certain range will not have great influence on the vibration characteristics. When the constraint stiffness is 10^8 N/m, the influence of 50% Euler critical load on the first-order frequency is less than 3%, and the high-order frequency is less than 1%. When the constraint of the elastic end of the beam is weak, the influence of the change of axial pressure is mainly reflected in the first mode shape. When the constraint stiffness is 10^4 N/m, the influence of the variation amplitude of the axial compression can reach more than 20%, while the influence of the variation amplitude of the higher order mode is small. The variation of the natural frequency of the second order mode is about 3%, and the variation amplitude of the third order mode is less than 1%.
(4) The elastic constraint value range with significant change in the natural frequency of the higher order mode is larger. When the first order frequency reaches $100EI/l^3$, the change tends to be flat, the second order frequency is about five times than that of the first order, and the third order frequency value range is 15 times or more.

Acknowledgements The authors gratefully acknowledge the financial supported by the National Natural Science Foundation of China (Grant No.51778035), Beijing Advanced Innovation Center for Future Urban Design (No. UDC2016030200) and The Fundamental Research Funds for Beijing University of Civil Engineering and Architecture (X19038), as well as Beijing Cooperative Innovation Research Center on Energy Saving and Emission Reduction.

References

1. Clough RW, Penzien J (1975) Dynamics of structures. McGraw-Hill
2. Bokaian A (1988) Natural frequencies of beams under compressive axial loads. J Sound Vibr 126(1):49–65
3. Banerjee JR, Ananthapuvirajah A (2019) Free flexural vibration of tapered beams. Comput Struct 224(Nov):106106.1–106106.6
4. Lee JW, Lee JY (2016) Free vibration analysis using the transfer-matrix method on a tapered beam. Comput Struct 164(FEB):75–82
5. Murtagh PJ, Basu B, Broderick BM (2004) Simple models for natural frequencies and mode shapes of towers supporting utilities. Comput Struct 82(20/21):1745–1750
6. Hu Z, Gao Q, Wang R et al (2014) Influence of axial load on natural vibration frequency of structure. Low Temp Architect Technol 36(012):75–78 (in Chinese)
7. Jafari A, Ezzati M, Atai AA (2018) Static and free vibration analysis of Timoshenko beam based on combined peridynamic-classical theory besides FEM formulation. Comput Struct 213
8. Chang JR, Lin RJ, Huang RJ et al (2010) Vibration and stability of an axially moving rayleigh beam. Appl Math Model 34(6):1482–1497
9. Li WL (2000) Free vibrations of beams with general boundary conditions. J Sound Vib 237(4):709–725
10. Lin LB, Wan YL, Jun D et al (2011) Vibration analysis of beams with arbitrary elastic boundary conditions. Appl Mech Mater 1326
11. Zhao Y, Du J, Xu D (2020) Vibration characteristics analysis for an axially loaded beam with elastic boundary restraints. J Vibr Shock 39(15):109–117 (in Chinese)
12. Bao S, Zhou J, Cao J, Shen F (2020) Free vibration analysis of foundation-beams with variable cross section and arbitrary elastic end-constraints. Chin J Appl Mech 37(05):2228–2234 + 2335–2336 (in Chinese)
13. Yang S, Wang T (2011) Nature frequency analysis of a cantilever beam with elastic restraint in vertical direction. J Tianjin Univ (Sci Technol) 44(001):18–22 (in Chinese)
14. Wang L (2013) Analysis of prestressing effect on nature frequency for simply supported beam. Jilin University (in Chinese)
15. Zhang Y, Lou M (2010) The modal characteristics analysis of wind turbine. Chin J Appl Mech (03):626–629 (in Chinese)